American Mineralogist, Volume 84, pages 447–453, 1999

^{57}Fe nuclear forward scattering of synchrotron radiation in hedenbergite $CaFeSi_2O_6$ at hydrostatic pressures up to 68 GPa

L. ZHANG,[1] J. STANEK,[2] S.S. HAFNER,[1,*] H. AHSBAHS,[1] H.F. GRÜNSTEUDEL,[3] J. METGE,[3] AND R. RÜFFER[3]

[1]Scientific Center of Materials Sciences and Institute of Mineralogy, University of Marburg, 35032 Marburg, Germany
[2]Institute of Physics, Jagiellonian University, 30-059 Cracow, Poland
[3]European Synchrotron Radiation Facility, 38043 Grenoble Cedex, France

ABSTRACT

The ^{57}Fe nuclear forward scattering (NFS) of synchrotron radiation and the use of diamond anvils with helium as pressure medium allowed study of the electronic state of Fe^{2+} in the chain silicate hedenbergite $CaFeSi_2O_6$ at pressures up to 68 GPa. Characteristics of NFS time spectra were compared with those of conventional Mössbauer spectra.

NFS time spectra of ^{57}Fe in hedenbergite revealed a reversible phase transition between 53 and 68 GPa at room temperature, which is probably a transition from the paramagnetic phase at low pressures to a magnetic phase at high pressures. If this interpretation is correct, the Néel temperature T_N of hedenbergite depends critically on pressure (T_N = 45 K at 1 atm).

INTRODUCTION

Development of powerful photon ''factories'' permit realization of Ruby's (1974) prediction of resonant nuclear absorption of synchrotron radiation (SR). The aim of this paper is twofold: first, the principles of nuclear forward scattering (NFS) at high pressures are described briefly. This part includes methodological considerations about the accuracy in determining nuclear hyperfine parameters from NFS data compared with those obtained from conventional transmission Mössbauer spectroscopy. Second, new results on the local electronic state of Fe^{2+} in hedenbergite $CaFeSi_2O_6$ at high pressures up to 68 GPa are presented.

NUCLEAR FORWARD SCATTERING

For our NFS experiments, SR of the nuclear resonance beam line (ID18) at the European Synchrotron Radiation Facility (ESRF) was used (see Rüffer and Chumakov 1997 for review). The duration t_p of the SR pulse was generally much shorter than the half life time τ of the ^{57}Fe first exited state, which was 98 ns. However, the time interval between pulses should be longer than, or at least comparable with τ. The storage ring at ESRF was operated in ''16 bunch mode,'' i.e., with 16 equally spaced bunches per revolution period. The SR pulses had a duration of about 100 ps and intervals of 176 ns between them. The SR from the undulator was monochromatized in a first step by a two bounce Si (111) face monochromator, providing an energy bandwidth of about 2.8 eV at 14.4 keV. The resulting radiation was monochromatized in a second step to a bandwidth of about 0.006 eV by a high-resolution monochromator, which consisted of two channel-cut silicon crystals of asymmetric (422) and symmetric (12,2,2) faces. The arrangement of the monochromators and high-pressure cell for the experiment is shown in Figure 1.

The maximum beam current of electrons in the ring was about 90 mA. The beam size of collimated SR from the high-resolution monochromator was about 0.4 mm × 2.0 mm. This beam was collimated by the sample hole of the rhenium gasket in the high-pressure diamond-anvil cell (DAC). In the detector system, the counts of the prompt electronic scattering and the delayed NFS pulses from the sample were recorded by a fast avalanche photodiode (Fig. 1). The delayed count rates from a sample without the DAC were e.g., about 230 counts/s with the DAC between 1 and 8 counts/s, depending on sample thickness. The accumulation time for one spectrum varied between 0.5 and 3 h. For a time spectrum (e.g., of hedenbergite in the DAC) the accumulation time was more than 100 times shorter than for a Mössbauer spectrum with comparable quality obtained from the same sample using B_4C anvils (10 mCi ^{57}Co source with 3 mm^2 active area) as described by Zhang and Hafner (1992).

While SR passes through the sample, ^{57}Fe nuclei are excited resonantly, without recoil, and decay afterward to the ground state. The decay curve $\mathbf{P}(t)$ is measured in a detector system and recorded in a multichannel analyzer as function $\mathbf{P}$ of the time from the excitation by SR pulse. From the shape of $\mathbf{P}(t)$ (which depends on the life time, splitting of the nuclear levels, and the effective thickness of the sample) the Mössbauer-Lamb factor and the hyperfine interaction parameters may be determined as described below.

* E-mail: hafner@mailer.uni-marburg.de

0003–004X/99/0003–0447$05.00

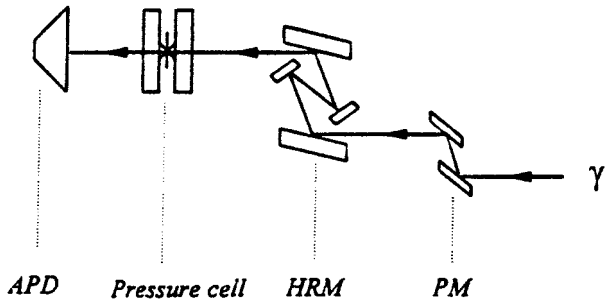

FIGURE 1. Arrangement of double reflection (PM) and high-resolution (HRM) monochromators, high-pressure cell, and fast avalange photodiode (APD) for nuclear forward scattering (NFS) experiment.

Let us consider the observed shape of $\mathbf{P}(t)$ in some detail. For this simple system with two levels of distinct but similar energies $E_1 = \hbar\omega_1$ and $E_2 = \hbar\omega_2$ (Fig. 2 insert) will be chosen. Such a system may refer, for example, to the two ^{57}Fe levels separated by nuclear quadrupole interaction at a crystallographic Fe position with lower than cubic point symmetry. Both levels that have been excited simultaneously will exhibit the same decay constant $\lambda = 1/\tau$. The decay curves $\mathbf{P}(t)$ of the two distinct levels will

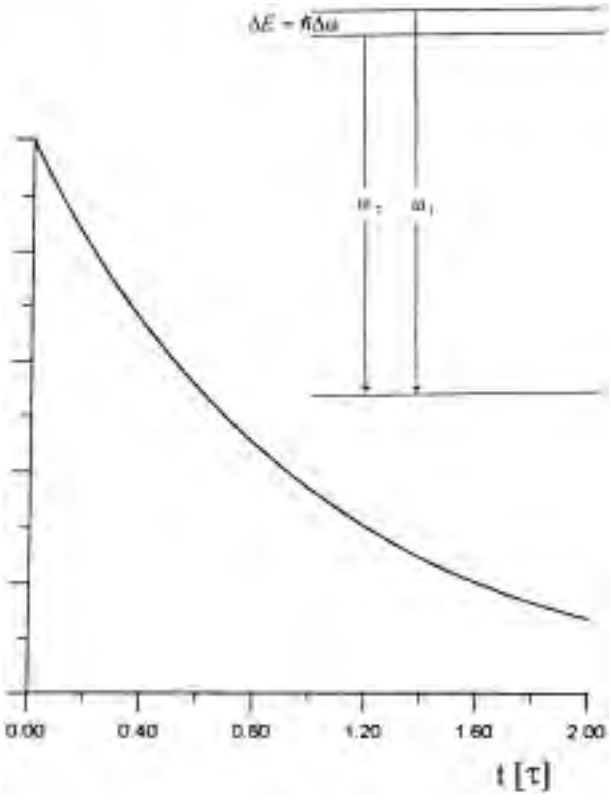

FIGURE 2. Decay curve $\mathbf{P}(t)$ for incoherent emission defined by Equation 1, for the energy level split shown in the inset. Here, ΔE is due to a ^{57}Fe quadrupole interaction at a Fe position of non-cubic point symmetry in a crystal.

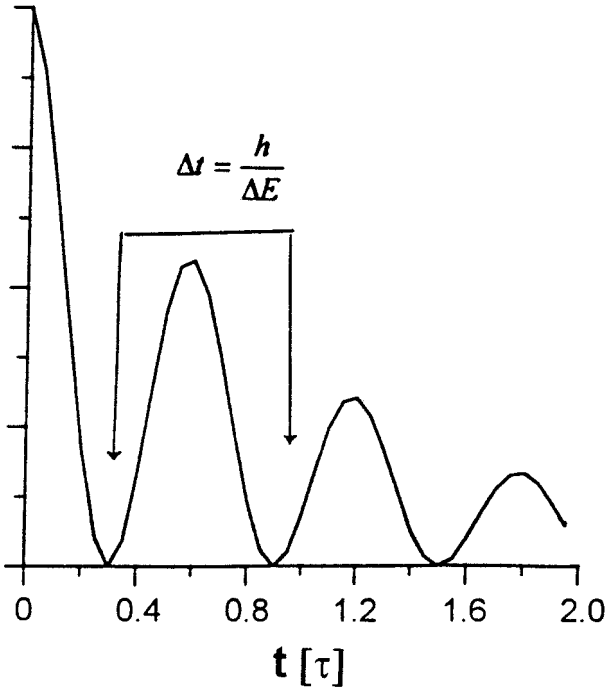

FIGURE 3. Decay curve $\mathbf{P}(t)$ for coherent emission defined by Equation 2 and the energy levels of Figure 2 inset.

depend on particular conditions. If in an experiment the energy level from which the transition originates is identified, the observed curve $\mathbf{P}(t)$ sketched in Figure 2 is the sum of $\mathbf{P}_1$ and $\mathbf{P}_2$, as follows:

$$\begin{aligned}\mathbf{P}(t) &= \mathbf{P}_1 + \mathbf{P}_2 \\ &= \left|\sqrt{\lambda}\, e^{-(\lambda t/2)} e^{-(i t\omega_1/2)}\right|^2 + \left|\sqrt{\lambda}\, e^{-(\lambda t/2)} e^{-(i t\omega_2/2)}\right|^2 \\ &= 2\lambda e^{-\lambda t}. \end{aligned} \quad (1)$$

However, NFS is a collective and coherent process. Therefore, it is not possible to assign the registered radiation to a particular level. The probability of decay at time t is the square of the sum of corresponding amplitudes ψ. This case is shown graphically in Figure 3 and presented in Equation 2.

$$\begin{aligned}\mathbf{P}(t) &= \left|\psi_1 + \psi_2\right|^2 \\ &= \left|\sqrt{\lambda}\, e^{-(\lambda t/2)} e^{-(i t\omega_1/2)} + \sqrt{\lambda}\, e^{-(\lambda t/2)} e^{-(i t\omega_2/2)}\right|^2 \\ &= 4\lambda e^{-\lambda t} \cos^2\left(\frac{\Delta\omega t}{2}\right), \end{aligned} \quad (2)$$

where $\Delta\omega = \omega_1 - \omega_2$ and ψ = amplitude. $\mathbf{P}(t)$ of Equation 2 exhibits periodical oscillations as shown in Figure 3. They are called ''quantum beats.'' The time between two neighboring minimums is $\Delta t = \hbar\Delta E$. Thus, from the decay curve, one may readily determine the energy level splitting, which is, in our case, the nuclear quadrupole splitting ΔE_Q of ^{57}Fe.

The considerations above correspond precisely to the case of particle diffraction at two slits as described in

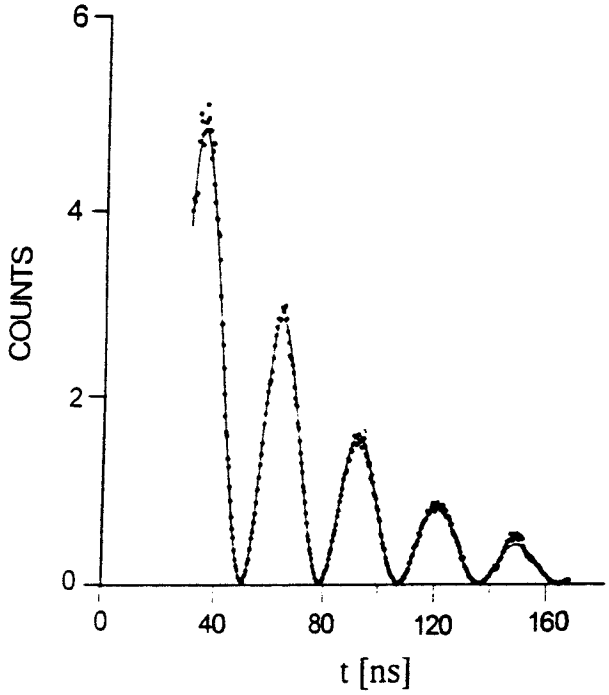

FIGURE 4. NFS time spectrum of ^{57}Fe in powdered forsterite $(Mg_{0.9975}Fe_{0.0025})_2SiO_4$, Fe enriched in ^{57}Fe to 97%. Time is in nanoseconds, the count rate in logarithmic scale. Areas exposed to Sr was 0.1 cm^2. Thickness was 0.1 mg ^{57}Fe/cm^2. Recording time was 0.5 h.

general physics for photons, electrons, or neutrons (Feynman et al. 1963). If the path of individual particles from the source through the slits to the screen cannot be measured, an interference pattern is obtained. The formal relationship between these two phenomena (oscillation of the decay curve due to split nuclear levels and particle diffraction at two slits) is indeed surprisingly close. In both cases, the interference effect follows from the uncertainty principle in form of $\Delta E \Delta t \geq \hbar$ and $\Delta p \Delta x \geq \hbar$, where Δp and Δx are the uncertainties in momentum and position, respectively. The limits between the two phenomena have been explored recently by Baron et al. (1996).

EVALUATION OF THE NFS TIME SPECTRUM

Nuclear quadrupole splitting ΔEQ in NFS time spectra

In general, interference methods are considered to be very accurate. ^{57}Fe in forsterite is a good example to illustrate the limits. In the crystal structure of forsterite, Fe^{2+} may substitute for Mg^{2+}, which occupies two non-equivalent positions, Mg1 and Mg2, with the point symmetries $\bar{1}$ and *m*, respectively. Both positions are octahedrally coordinated, the geometrical deformation of the $Fe^{2+}O^{2-}_6$ octahedra from regular symmetry being very similar. Therefore, two quite similar ΔE_Q values for Fe^{2+} are expected. In fact, because the two distinct splittings depend somewhat differently on temperature, they can be resolved at

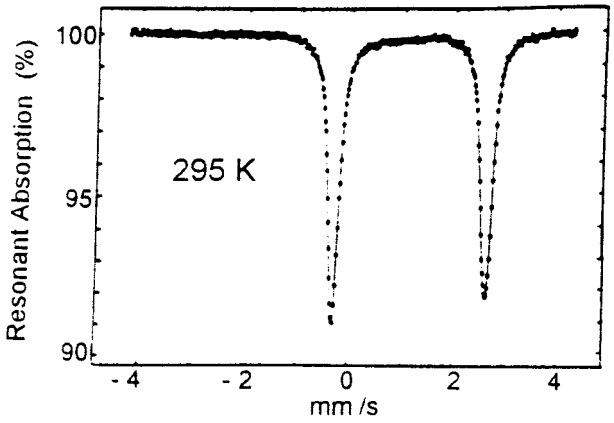

FIGURE 5. Conventional Mössbauer velocity spectrum of ^{57}Fe in forsterite $(Mg_{0.9975}Fe_{0.0025})_2SiO_4$, Fe enriched in ^{57}Fe to 97% (same sample as for the NSF time spectrum in Fig. 3). Although there is not any visible resolution of Fe^{2+} at the Mg1 and Mg2 positions the spectrum does not show resolution at temperatures above 540 K.

temperatures higher than about 250 °C (Stanek et al. 1986; Figs. 2 and 4). At ambient conditions, however, the distinction cannot be detected easily by simple inspection. Figures 4 and 5 show the time and conventional velocity spectra of the same powdered synthetic forsterite $(Mg_{0.9975}Fe_{0.0025})_2SiO_4$, enriched in ^{57}Fe to 97%, respectively. Least square fits to both spectra yielded distinct values for the Fe^{2+} quadrupole splittings Δ1 at Mg1 and Δ2 at Mg2 as well as the difference between the isomer shifts δ1 at Mg1 and δ2 at Mg2 (Table 1).

Magnetic splitting in NFS time spectra

Obviously, for a more complex energy level scheme which allows more than two transitions with different probabilities, the shape of $\mathbf{P}(t)$ may be quite puzzling. Figure 6 shows the ^{57}Fe time spectrum of hematite α-Fe_2O_3 with the six principal transitions. In hematite, the four magnetically split energy levels of the ^{57}Fe first excited state are not equidistant. They are perturbed by simultaneous ^{57}Fe quadrupole interaction. In this particular case where the quadrupole interaction is small compared

TABLE 1. Comparison of conventional Mossbauer spectroscopy and NFS of SR for Fe^{2+} at Mg1 and Mg2 in forsterite $(Mg_{0.9975}Fe_{0.0025})_2SiO_4$

	Mossbauer velocity spectrum*	NFS time spectrum†
Δ1 (Mg1)	2.920 (3)	2.91 (4)
Δ2 (Mg2)	3.105 (3)	3.07 (4)
δ1–δ2‡	0.009 (5)	0.02 (1)

Notes: Δ1 and δ2 = ^{57}Fe nuclear quadrupole splittings. δ1 and δ2 = isomer shifts.

* Stanek et al. (1986). Recording time was 71 h. Exposed area 1.1 cm^2; 0.2 mg ^{57}Fe/cm^2.

† This work. Recording time was 0.5 h; exposed area 0.1 cm^2; thickness 0.1 mg ^{57}Fe/cm^2.

‡ Difference between the isomer shifts δ at the M1 and M2 positions.

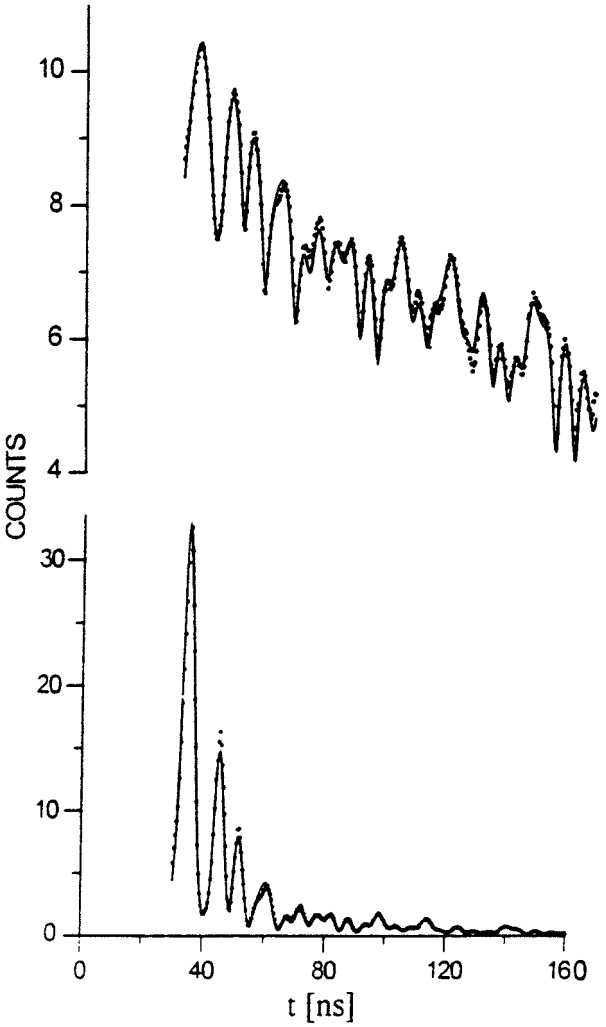

FIGURE 6. NFS time spectrum of ^{57}Fe in hematite α-Fe_2O_3: The count rate of the lower spectrum is a linear scale, that of the upper spectrum is a logarithmic scale.

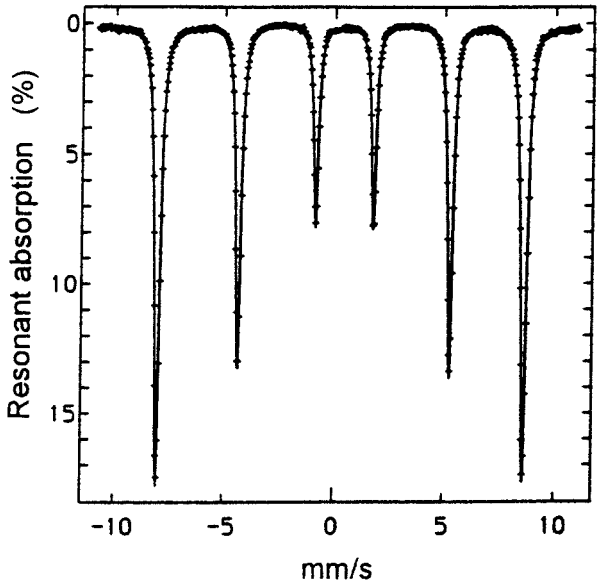

FIGURE 7. Conventional Mössbauer velocity spectrum of ^{57}Fe in hematite α-Fe_2O_3.

to the magnetic interaction, the splittings may be calculated readily by simple second-order perturbation theory without need of solving a mixed Hamiltonian (Hafner et al. 1967). The time spectrum in Figure 6 may be compared with the Mössbauer velocity spectrum of hematite shown in Figure 7.

Effect of sample thickness

The shape $\mathbf{P}(t)$ of the NFS time spectrum depends critically on the effective thickness d_s of the sample due to multiple scattering. It shows up as so called ''dynamical beats'' or ''Bessel beats.'' It should be noted that the shape of $\mathbf{P}(t)$ is quite different from the shape of conventional Mössbauer resonant absorption in the velocity spectrum. In general, absorber thickness $d_s = n\sigma_0 f$, where n is the number of ^{57}Fe nuclei per cm^2, σ_0 is the cross section for resonant nuclear absorption, $f = \exp[-4\pi^2\langle x^2\rangle/\lambda^2] = \exp[-2W]$ is the recoil-free fraction of ^{57}Fe, and W is the Lamb-Mössbauer factor (e.g., Greenwood and Gibb 1971) or ''Debye-Waller'' factor, $\langle x^2\rangle$ is the mean square vibrational amplitude of the nucleus, and λ is the wave length of the γ quantum. The thickness effect may be illustrated by a NFS experiment with a stainless steel absorber combined with simulation. In Figure 8, the time spectrum of a stainless steel foil enriched in ^{57}Fe to 97% is shown. The effective thickness d_s of that foil ($d \cong 1.6$ μm) was not homogeneous. The resulting spectrum was, therefore, quite broadened. It could be satisfactorily fitted adopting a Gaussian distribution of d_s with a variation over 10%. In Figure 9, theoretical spectra of stainless steel calculated for values $d = 0.1$ μm, 1.0 μm, and 2.0 μm, as well as for a significant Gaussian distribution near $d = 1.5$ μm, are presented to illustrate the effect of inhomogeneous sample thickness. For the calculations, Fe was assumed to be in enriched in ^{57}Fe to 97%. The particular sensitivity of NFS time spectra on d_s allows for accurate determination of f. However, it requires generally extreme care during sample preparation, especially when samples with Fe enriched in ^{57}Fe are studied.

Statistical background

In conventional Mössbauer spectroscopy, an appropriate γ energy range is selected from the energy spectrum of the source, typically with a single channel analyzer. The window (e.g., for ^{57}Fe resonance) may be chosen so that lower energy radiation such as the 6 keV X-rays, and higher energy radiation, such as the 122 keV and 136 keV γ-rays from the decay of the ^{57}Fe second excited state, are filtered. However, a significant amount of off-resonance pulses are superimposed to the 14.4 keV recoil-free resonant absorption. This ''background'' consists of

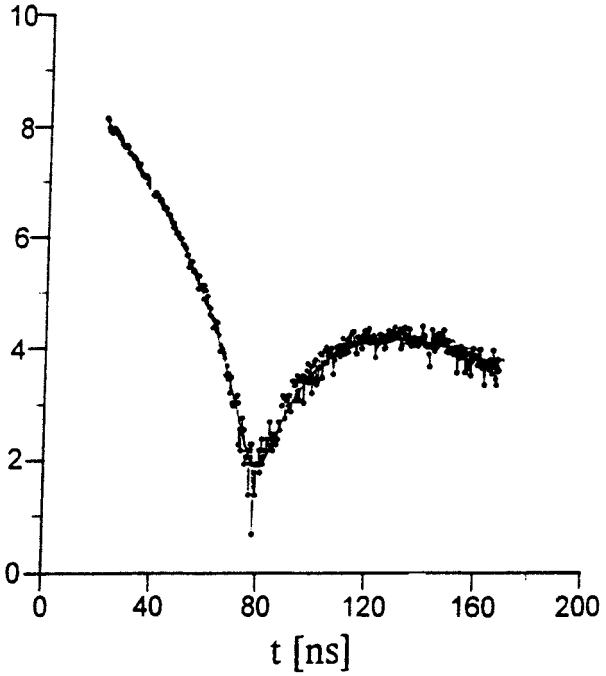

FIGURE 8. NFS spectrum of stainless steel foil with a thickness $d = 1.6$ μm enriched in ^{57}Fe to 97%. The count rate is in logarithmic scale.

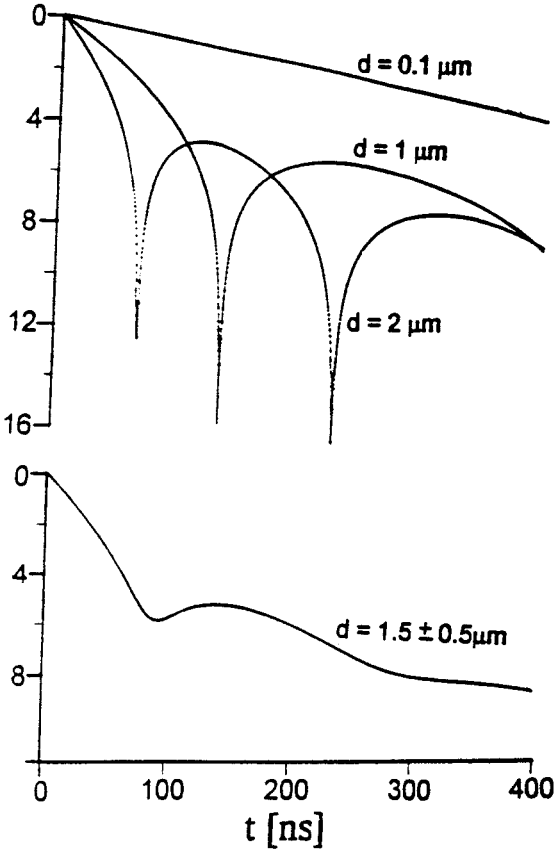

FIGURE 9. Simulation of NFS time spectra for stainless steel enriched in ^{57}Fe to 97% with three different thicknesses: $d = 0.1$ μm, $d = 1.0$ μm, and $d = 2.0$ μm. The ^{57}Fe nuclear levels in stainless steel are not split. The lowest curve simulated for a variable thickness with $1.2\ \mu m \leq d \leq 1.8\ \mu m$ illustrates the influence of variable thickness assuming Gaussian distribution. Scale is logarithmic.

(1) the fraction of 14.4 keV radiation, reduced by recoil energy, $(1 - f)$, and degraded high-energy radiation from the decay of the ^{57}Co source to the ^{57}Fe second and first excited states by Compton effect or Bremsstrahlung, produced by fast electrons present in the source. The superimposed fraction due to high-energy radiation from the decay comprises typically about 20% of the total 14.4 keV count rate.

NFS time spectra are free of non-resonant background, with the exception of the natural background in the laboratory, which should be negligible. The delayed counts recorded result exclusively form the decay of the ^{57}Fe first excited state (Fig. 4). In conventional Mössbauer spectra, background and experimental line width are fitted by free, adjustable parameters (Figs. 5 and 7). In our fits of simple NFS time spectra, these parameters were not necessary.

Fitting of NFS time spectra

The NFS time spectra were fitted by use of the programs of Sturhahn and Gerdan (1994) as well as Shvyd'ko (1996). Variable parameters in the free fit were ΔE_Q, local magnetic field H_0 in case of magnetic splitting, absorber thickness d_s, and isomer shift δ referred to metallic iron. δ was calibrated with a stainless steel calibration foil enriched in ^{57}Fe to 97%. A Gaussian distribution of absorber thickness was assumed.

NFS at high pressures

DACs designed generally for high-pressure X-ray diffraction were used to generate high pressures up to 68 GPa. The culets of the two diamonds were 600 μm for pressures up to 20 GPa and 300 μm for pressures up to 70 GPa. Rhenium gaskets with sample holes that had diameters between 400 and 145 μm were used for collimating the 14.4 keV radiation. The sample was prepared in form of a disk with a diameter between 250 and 110 μm and a varying thickness between 20 and 40 μm, yielding effective thicknesses d_s between 30 and 60 μm. It was placed on the culet without bonding material. Three to five grains of ruby were placed around the sample disc, and the pressure distribution was determined by the shift of ruby fluorescence lines.

The DAC was loaded in a steel gas pressure vessel in which helium gas was pressurized to approximately 0.2 GPa. Previous single crystal diffraction studies (Zhang and Ahsbahs in preparation) revealed superior hydrostatic conditions of helium as a pressure medium up to more than 30 GPa. Hydrostatic conditions are essential for reducing complexity in the evaluation of the spectra. The pressure gradient measured at 68 GPa, which was the

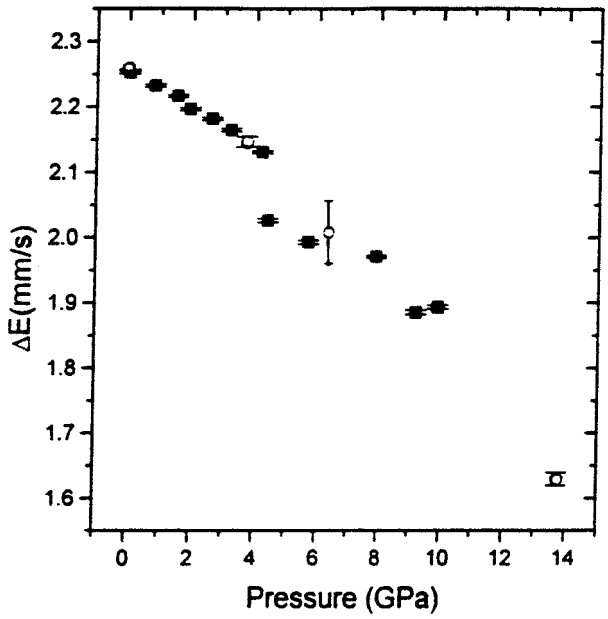

FIGURE 10. ΔE_Q values. Solid squares refer to conventional Mössbauer velocity spectra (Zhang and Hafner 1992). Open circles to NFS time spectra at 0, 3.7, 5.9, and 13.7 GPa. The estimated total errors are indicated.

highest pressure attained in this experiment was 2 GPa across the sample area.

NFS TIME SPECTRA OF HEDENBERGITE UP TO 68 GPA

A synthetic polycrystalline sample of hedenbergite $CaFeSi_2O_6$ with Fe enriched in ^{57}Fe to 92.2% was synthesized at 600 °C and 0.1 GPa H_2O vapor pressure over a period of seven days and tested with X-ray diffraction, as well as conventional ^{57}Fe Mössbauer spectroscopy. No foreign phase was observed within the limit of detection. That same sample was used previously (Zhang and Hafner 1992) in conventional ^{57}Fe study at pressures up to 10 GPa with B_4C anvils and paraffin as the pressure transmitting medium.

In a first series, NFS time spectra were recorded at pressures of 3.7 GPa, 5.9 GPa, and 13.7 GPa twice—first without and second with the stainless steel calibration foil. This procedure enabled independent determination of δ and ΔE_Q. The ΔE_Q values obtained from the spectra (Fig. 10) are in good agreement with those measured previously by Zhang and Hafner (1992). The greater experimental errors of the time specta compared to those of the conventional spectra must be considered in terms of the much smaller absorber areas in the diamond anvils, compared to the B_4C anvils and the recording times that were more than 100 times less for the NFS time spectra than those for the conventional spectra of Zhang and Hafner (1992).

In a different DAC with smaller culets, time spectra were recorded at 53.3 GPa (not shown) and 68 Gpa (Fig. 11). The significant change compared to a spectrum with the typical quadrupole splitting (e.g., Fig. 4) should be noted. Between these two pressures, a phase transition must occur, which was found to be reversible, at least from the NFS spectra. The time spectrum after pressure release exhibited the same δ and ΔE_Q values as the original sample before the high-pressure runs.

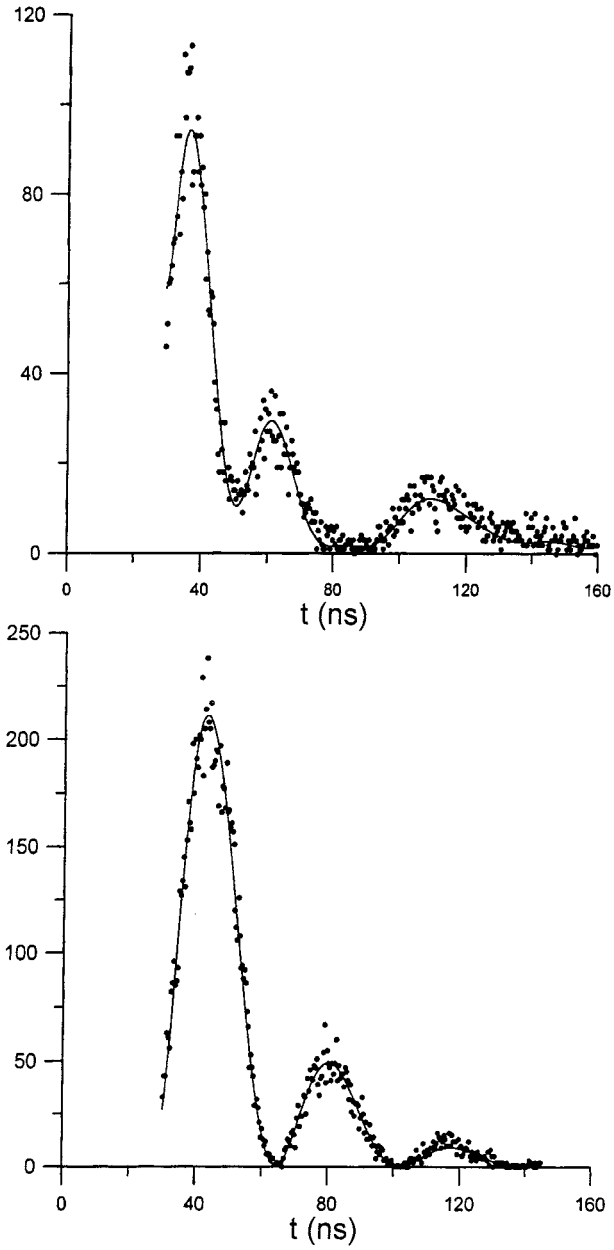

FIGURE 11. (Above) NFS spectrum of hedenbergite at 68 GPa. The solid line is the fit assuming the mixed magnetic-quadrupole interaction. Note the different distances between maximums that excludes pure quadrupole interaction. **(Below)** NFS spectrum of the same sample (in the DAC) taken at 0 GPa after releasing pressure.

Discussion

The ΔE_Q values determined from the time spectra of hedenbergite at low pressure (Fig. 10) are in good agreement with the linear dependence of δ and ΔE_Q on pressure between 0 and 4 GPa. They were consistent with the discontinuity at 4 GPa described by Zhang and Hafner (1992).

The time spectra recorded at 53.3 GPa and 68 GPa revealed a significant difference in their shapes. This change must be related to a new phase transition. Although the spectrum at 53.3 GPa resembles qualitatively to those at lower pressures it could not be fitted using appropriate hyperfine parameters, probably because the pressure was near that of the transition.

Inspection of the spectrum above the transition (Fig. 11) showed that the parameters of the spectra at pressures below the transition could not be used as initial set for a fit. In a first approach, it was fitted with a large number of arbitrary lines until the fit became statistically acceptable ($\chi^2 < 1$ for 12 lines). Then the fit was transformed to a conventional Mössbauer velocity spectrum. That procedure allowed insight in the spectral structure based on magnetic and paramagnetic spectra of pyroxene-type chain silicates above and below the Néel point known to date (Wiedenmann et al. 1986; Stanek et al. 1986, and references cited there).

Finally the spectrum was fitted by use of the Hamiltonian for the general case of mixed electrostatic and magnetic interaction. The final hyperfine values obtained in this way were $H_0 = 66 \pm 0.5$ kOe, $\Delta E_Q = 1.2 \pm 0.2$ mm/s, the asymmetry parameter of tensor V_{ii}, $\eta = V_{xx}/(V_{yy} - V_{zz}) = 0.6 \pm 0.2$, the angle θ between H_0 and V_{zz} $\theta = 30 \pm 10°$. The angle φ between the projection of $\mathbf{H}_0$ on the *XY* plane was constrained to be $\varphi = 0$. The isomer shift δ was not determined. Such a complex procedure must produce large systematic errors. The values above are nevertheless quite reasonable in view of the values known from previous experimental studies of ^{57}Fe in pyroxenes at ambient pressure (Wiedenmann et al. 1986; Stanek et al. 1986).

Although additional study is needed for a more complete analysis of the transition to a magnetic phase between 53.3 GPa and 68 GPa, several arguments do support its existence. Orthoferrosilite $Fe_2Si_2O_6$ shows ferromagnetic alignment of the Fe^{2+} magnetic moments below the Néel Temperature $T_N = 45$ K, the $Fe^{2+}O_6$ octahedral ribbons being antiferromagnetically coupled. Hedenbergite is also magnetically ordered below $T_N = 41$ K (Hafner, unpublished data). If the transition between 53 GPa and 68 GPa is indeed a magnetic transition similar to the one observed at 41 K, T_N must depend critically on pressure. The precise magnetic structure of hedenbergite is not yet known but is likely to be similar to that of iron-rich orthopyroxene (Wiedenmann et al. 1986). The paramagnetic time spectrum obtained at ambient pressure after pressure release is indicative of a reversible transition between 53 GPa and 68 GPa. It excludes a reconstructive transition. Furthermore, it cannot be the Fe^{2+} high spin $\leftrightarrow$ low spin transition as predicted by Lin et al. (in preparation) to occur at about 50 GPa from theoretical crystal field calculation even though such transition may be possibly associated with a substantial change in chemical bonding of the silicate.

Acknowledgments

We thank Bernhard Seeger for programming advice and Gertrud Steinbach for technical assistance.

References cited

Baron, A.Q.R., Shumakov, A.I., Grünsteudel, H.F., Grünsteadel, Hanna, Niesen, L., and Rüffer, R. (1996) Traverse x-ray coherence in nuclear scattering of synchrotron radiation. Physical Review Letters, 77, 4808–4811.

Feynman, R.P., Leighton, R.B., and Sands, M.L. (1963) Feynman Lectures on Physics, Addison-Wesley Publishing Company, Inc., Massachusetts, U.S.A.

Greenwood, N.N. and Gibb, T.C. (1971) Mössbauer spectroscopy. Chapman and Hall, London.

Hafner, S.S., Evans, B.J., and Kalvius, G.M. (1967) Second-order effects in the hyperfine field of Fe^{57} in troilite (antiferromagnetic FeS). Solid State Communications, 5, 17–19.

Ruby, S.L. (1974) Mössbauer experiments without conventional sources. Journal de Physique Colloque, C6, 35, 209–211.

Rüffer, R. and Chumakov, A.I. (1997) Recent trends in nuclear resonance scattering. In E.A. Görlich and K. Latka, Eds., Proceedings of the XXXII Zakopane School of Physics, Zakopane, Poland, 10–17 May 1997.

Shvyd'ko, Yu. (1996) Motif: a program for fitting Mössbauer time spectra of nuclear forward scattering. Zweites Institut für Experimentalphysik, Universität Hamburg, version of 1996.

Stanek, Jan, Hafner, S.S., and Sawicki, J.A. (1986) Local states of Fe^{2+} and Mg^{2+} in magnesium-rich olivines. American Mineralogist, 71, 127–135.

Sturhahn, W. and Gerdau, E. (1994) Evaluation of time differential measurements of nuclear resonance scattering of X-rays. Physical Review B Condensed Matter, 49, 9285–9294.

Wiedenmann, A., Regnard,, J.R., Fillion, G., and Hafner, S.S. (1986) Magnetic properties and magnetic ordering of the orthopyroxenes $Fe_xMg_{1-x}SiO_3$. Journal of Physics C, Solid State Physics, 19, 3683–3695.

Zhang, Li and Hafner, S.S. (1992) High-pressure ^{57}Fe γ resonance and compressibility of $Ca(Fe,Mg)Si_2O_6$ clinopyroxenes. American Mineralogist, 77, 462–473.

Manuscript received June 23, 1998
Manuscript accepted October 30, 1998
Paper handled by John Parise